### Martin Hähsler, Ingo Appel and Silke Behrens\*

# Magnetic hybrid materials in liquid crystals

**Abstract:** The integration of nanoparticles with magnetic, ferroelectric or semiconducting properties into liquid crystals (LCs) has attracted great interest both for fundamental investigations and for technological applications. Here, an overview of hybrid materials based on magnetic nanoparticles (MNPs) and thermotropic LCs is given. After a general introduction to thermotropic LCs and LC-MNP hybrid materials, various preparation methods established by us are presented. The synthesis of shape-(an)isotropic MNPs, their functionalization by tailored (pro)mesogenic ligands with linear or dendritic structures and their integration into LC hosts are discussed. The characterization of the MNPs, (pro)mesogenic ligands and resulting MNP-LC hybrid materials is described to show the influence of MNP functionalization on the MNP-LC interactions including aspects such as colloidal stability and structuring in the LC host. Overall, we show that the physical properties of the hybrid material are significantly influenced not only by the MNPs (i.e., their size, shape and composition) but also by their surface properties (i.e., the structure of the (pro)mesogenic ligands).

**Keywords:** inorganic/organic hybrid materials, magnetic nanoparticles, magneto-optical properties, nematic liquid crystals, (pro)mesogenic ligands

## 1 Introduction

The integration of nanoparticles with magnetic, ferroelectric or semiconducting properties in liquid crystals (LCs) has attracted a lot of interest for both fundamental investigation and technological application [1]. Long-distance orientational interaction in LCs leads to a strong influence of the dispersed particles on the mesogenic properties of the LC and *vice versa*. In general, two major directions are pursued (1) the LC host directs the organization of the particles into ordered arrays with synergistic collective behaviors or (2) the particle dopants modulate and improve the properties of the LC. Dopants of magnetic nanoparticles (MNPs) can effectively modify the electroand/or magneto-optical responses and other physical characteristics of LCs. These

<sup>\*</sup>Corresponding author: Silke Behrens, Institute of Catalysis Research and Technology, Karlsruhe Institute of Technology, Postfach 3640, 76021 Karlsruhe, Germany; and Institute of Inorganic Chemistry, Ruprecht-Karls University Heidelberg, Im Neuenheimer Feld 270, 69120 Heidelberg, Germany, E-mail: silke.behrens@kit.edu, https://orcid.org/0000-0003-4328-9564

Martin Hähsler and Ingo Appel, Institute of Catalysis Research and Technology, Karlsruhe Institute of Technology, Postfach 3640, 76021 Karlsruhe, Germany; and Institute of Inorganic Chemistry, Ruprecht-Karls University Heidelberg, Im Neuenheimer Feld 270, 69120 Heidelberg, Germany

hybrid materials reveal a great potential to improve current liquid crystal display (LCD) technologies, for example, through new or modified switching modes, lower operating voltages and larger contrast-ratios [2]. Recently, hybrid materials of LCs and MNPs with magnetically controllable and erasable characteristics (in particular magneto-chromic properties) were developed which could be interesting for application as magnetic paper [3]. Magnetic fields could be directly visualized by combining the magneto-optical and electro-optical response of ferromagnetic LCs [4]. Polymeric LCs have also been doped with MNPs which allows for their mechanical deformation or heating by the action of external (magnetic) stimuli [5]. Transparent magnets with flexible and optically homogeneous properties, for example, were achieved by linking polymeric, side-chain LCs with a siloxane backbone to MNPs [6].

LCs thermodynamically range between the highly ordered crystalline and disordered isotropic liquid state and are therefore often referred to as mesophase (Figure 1a). This mesophase combines anisotropic properties of crystals (such as optical birefringence) with flow properties of ordinary liquids. Anisotropic properties arise from ordering of constituent entities, while fluid properties are provided by their concomitant mobility in LC state. In general, molecules, macromolecules, supramolecular aggregates or nanoparticles may act as constituent entities in LCs. Here, we focus on LCs formed by low-molecular weight molecules. Depending on the mesophase, LCs are classified into two categories, namely thermotropic and lyotropic LCs. Lyotropic LCs can be found in solutions of amphiphilic molecules forming micellar aggregates, where concentration largely determines the type of LC phase formed. In thermotropic LCs, LC ordering is a function of temperature (Figure 1a). Thermotropic LCs are formed by single organic molecules as constituent entities (i. e. mesogens) or mixtures thereof,

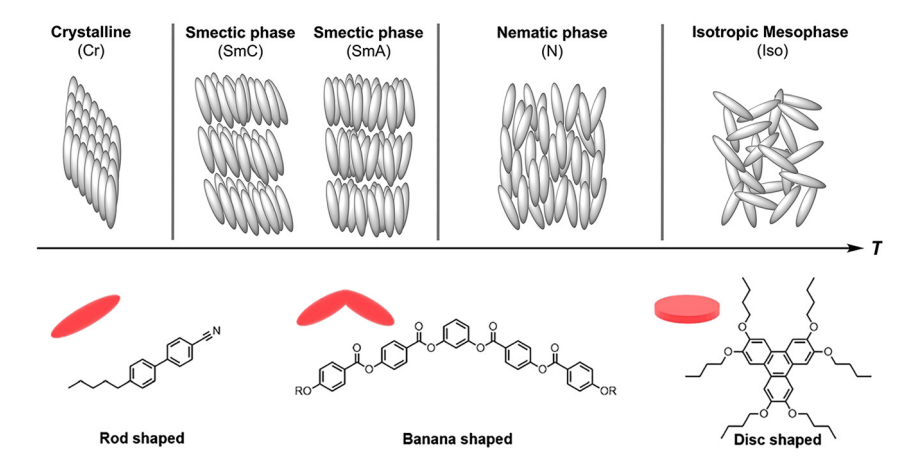


Figure 1: (a) Organization in the crystalline, liquid crystal (LC) and liquid state with common LC phases formed by calamitic mesogens. (b) Selected structures of mesogens forming LCs.

which are further distinguished according to the geometric shape into calamitic (rodlike), discotic (disc-like), sanidic (brick-like or lath-like) or bent-core (Figure 1b) [7]. LCs are symmetry-broken, ordered fluids in which one or more angular and/or positional degrees of freedom are frozen in. While mesogens in nematic mesophases show longrange, orientational ordering along a preferred direction (director n), they additionally reveal positional ordering in smectic phases. Various types of thermotropic mesophases occur at different temperatures; some common types formed by calamitic mesogens are displayed in Figure 1b [7].

Already in the 1970s, Brochard and de Gennes proposed the embedding of MNPs into LC hosts to increase the magnetic response or sensitivity, respectively, of LCs to magnetic fields [8]. Meanwhile, a number of lyotropic and thermotropic MNP-LC hybrids with interesting magneto-optical properties have been realized experimentally [9]. In this context, ferronematics represent stable colloidal suspensions of MNPs in nematic LCs. Mertelj et al. have reported on ferromagnetic nematics by the stabilization of ferromagnetic Sc-doped barium hexaferrite platelets in the nematic LC 4-pentyl-4'-cyanobiphenyl (5CB) [10]. The interplay of nematic-mediated repulsive interaction and magnetic attraction forces lead to stabilization of the MNPs and their ferromagnetic ordering in the LC [11]. Multiferroic properties were achieved due to the coupling of the nematic director n and the magnetization M of the platelets [12]. The electro-optical effect of the ferromagnetic LC, which did not differ from the pure LC, was accompanied by an opposite magneto-electric and an (indirect) magneto-optical effect. The birefringence of LCs consisting of shape-anisotropic organic pigments was controlled by MNPs forming chain-like structures in the magnetic field [13]. As shown by molecular dynamic simulations, the size and number of chain-like MNP clusters determined the alignment of these pigments [14]. Recently, Stannarius, Schmidt and Eremin et al. also demonstrated the magneto-optical response of isotropic and anisotropic fibrillous organogels by mobile MNPs [15]. Orientational ordering is known not only to affect the electro-optical but also the rheological properties of colloidal dispersions. Nematics, for example, reveal a complex flow behavior which depends on the flow direction and type and involves different viscosities (so-called Leslie coefficients). In this case, magneto-viscous effects which have been described for ferrofluids could also open up novel possibilities for MNP dispersions in LC hosts [16]. Just recently, an interesting magneto-viscous effect was observed by Odenbach et al. for doping of isotropic, micellar potassium laurate/water systems with MNPs [17]. The ternary mixture (potassium laurate/water/decanol) also forms a lyotropic mesophase which could give rise to interesting magneto-rheological properties [18]. In an LC mixture of magnetic and nonmagnetic nanorods, a nonmonotonic dependence of the shear stress on the strength of an external magnetic field was observed by molecular dynamics simulations, which is in contrast to the monotonic behavior in conventional ferrofluids [19]. Recently, translational and rotational motions of ferromagnetic liquid droplets were

precisely actuated by an external magnetic field [20]. The droplets could be reconfigured into different shapes while preserving the magnetic properties of solid ferromagnets with classic north-south dipole interactions. Here, the droplets were built from isotropic phases and MNP-surfactants, but this could also inspire future studies on active matter and programmable liquid constructs based on MNP-LC hybrids.

However, the embedding of particles in LC matrices is by no means trivial. As shown by us and others, aggregation of MNPs up to the complete phase separation is highly challenging. The stability of MNP dispersions is typically low, and formation of aggregates often occurs even in colloids with low MNP content. In some cases, the stability of the colloidal LC dispersion seemed to be hardly longer than the measurement time of the experiments. Visible to the eye, macroscopic MNP precipitates may rapidly form below the isotropic-nematic transition leading to a spontaneous, complete phase separation into colorless LC phase and brown MNP precipitate. MNP dispersions, however, can also appear macroscopically homogeneous below the isotropic-nematic transition, whereby no precipitate is formed, while examination with the optical microscope reveals the formation of (micro)aggregates [10, 21]. Even microaggregate formation may affect the magneto-optical behavior of MNP dispersions in LCs, as demonstrated by polarizing microscopy (POM) in the magnetic field [22]. Local response of the director  $\mathbf{n}$  near the MNP microaggregates orienting in the magnetic field led to a first nonthreshold region of the phase retardation, while the collective response of the LC with the homogeneously dispersed MNPs occurred at larger magnetic fields (≥95 mT). MNP aggregates may be removed, for example, applying an external magnetic field gradient (Nd<sub>2</sub>Fe<sub>14</sub>B laboratory magnet), which leads to colloidally stable MNP dispersions where no aggregates are detected by optical microscopy [21]. However, this may not exclude the formation of small MNP clusters well dispersed in the LC and not visible under the optical microscope [23]. In particular high MNP fractions may also affect the LC viscosity and thereby the fluidity of the sample, and even gelatinous nonfluid materials have been reported for high MNP fractions [22]. Preparation procedures made also use of rapid thermal quench (i. e., by rapid cooling from the isotropic to the nematic phase) to keep the particles, which are in general better dispersible in the isotropic liquid phase, from aggregating in the nematic phase [24].

In general, a stabilization of MNPs in LCs requires not only the compatibility of the particles with the structure and dimensions of the LC host as well as specific surface properties, but also a balanced interplay of LC-mediated and magnetic forces that might occur. The coating of the MNPs with tailored (pro)mesogenic ligands is very promising, particularly for stabilizing MNPs in thermotropic LCs. For particles of semiconductors or metals (in particular small Au nanoparticles [25] and nanorods up to 50 nm [26]), the use of (pro)mesogenic ligands has been successfully demonstrated. Desymmetrization by replacing spherical Au particles by nanorods as well as the coating with chiral ligands, induced a much tighter helical distortion and an amplification of chirality in the LC host [26]. The functionalization of ZnO nanoparticles, spindle-shaped TiO<sub>2</sub> and α-Fe<sub>2</sub>O<sub>3</sub> particles with (pro)mesogenic ligands is also described [27]. Surprisingly, only few examples describe the use of (pro)mesogenic ligands for stabilization of MNPs in LCs. As compared to oleic acid-stabilized nanorods, nanorods coated with 4-n-octyloxybiphenyl-4-carboxylic acid revealed an enhanced stability in 5CB [91]. (Pro)mesogenic ligands with dendritic structure are particularly interesting and were first exploited for the functionalization of MNPs by Dermortière et al. [28]. Recently, stable dispersions of CdSe@ZnS quantum dots and MNPs were also achieved in 5CB by using dendritic ligands [22, 25c, 29].

In the following, we give an overview on the synthesis of MNPs of various elemental compositions and defined spherical or anisotropic shape as well as their integration in low-molecular weight LCs. We report on the synthesis of various (pro) mesogenic ligands and the successive surface engineering of the MNPs for preparing stable colloidal dispersions in nematic LCs.

## 2 Discussion

# 2.1 Size and shape-controlled synthesis of magnetic nanoparticles (MNPs)

In general, the magnetic properties of MNPs depend on their size, shape and elemental composition. The size, shape, topology and the magnetic properties of the MNPs are very important because they determine the interactions between the particles inserted into a medium that is partially ordered such as a nematic LC. Various synthetic methods are available to prepare uniform MNPs with a defined size, shape and various elemental compositions, including co-precipitation [21], thermal decomposition [30], microemulsion [31] and hydrothermal/solvothermal [32] synthesis. Exemplary MNPs of various sizes, shapes and elemental compositions which were obtained here are depicted in Figure 2 [18].

Bulk CoFe<sub>2</sub>O<sub>4</sub> displays an inverse spinel structure, a high chemical and physical stability together with an unusually high magnetocrystalline anisotropy ( $\sim 2 \times 10^5 \text{ J/m}^3$ ). Electrostatically stabilized CoFe<sub>2</sub>O<sub>4</sub> MNPs, for example, were obtained via coprecipitation of the Co<sup>2+</sup> and Fe<sup>3+</sup> salts [21, 33]. A NaOH solution was injected into the vigorously stirred, acidic solution of the Co<sup>2+</sup> and Fe<sup>3+</sup> precursors to yield ultrasmall uniform  $CoFe_2O_4$  MNPs with a particle size of 2.5 ( $\pm 0.6$ ) nm. As these MNPs were electrostatically stabilized, the (pro)mesogenic ligands could be directly bound to the MNP surface, and no ligand exchange was required. The functionalization of MNPs is discussed in detail below. Thermal decomposition of  $Co(acac)_2$  and  $Fe(acac)_3$  yielded 7.4 ( $\pm 0.9$ )-nm-sized Co<sub>0.6</sub>Fe<sub>2.4</sub>O<sub>4</sub> MNPs stabilized by oleyl amine/oleic acid by modifying a procedure originally described by Sun et al. (Figure 2a) [30a]. The shape of the MNPs is another important aspect, and particles with shape anisotropy are of particular interest. While size (and composition) determines superparamagnetic or magnetically blocked

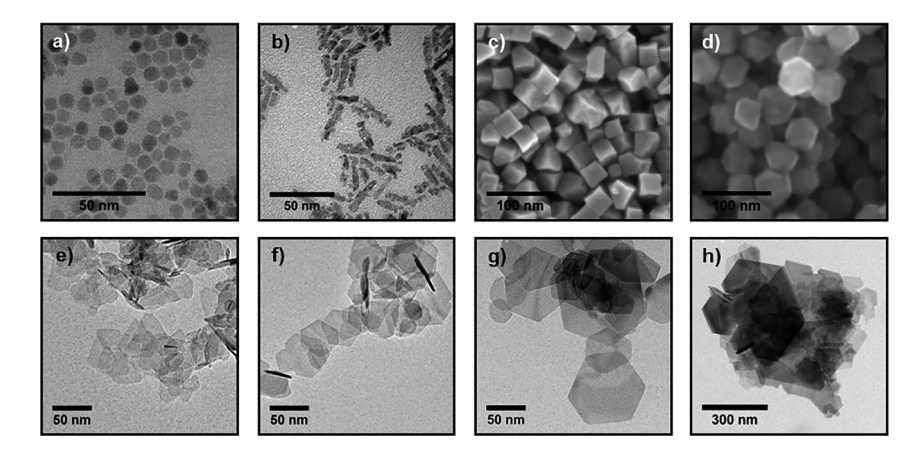


**Figure 2:** Transmission electron microscopy micrographs of (a) spherical  $Co_{0.6}Fe_{2.4}O_4$  MNPs (7.4 (±0.9) nm) and (b)  $Fe_3O_4$  nanorods (dimensions 27.0 (±9.1) × 5.5 (±1.0) nm). (c)–(d) scanning electron microscopy images of (c) nanocubes (edge length 27.0 (±3.0) nm) and (d) cuboctahedra with a particle size of 37.5 (±5.7) nm. (e)–(h) TEM micrographs of scandium-doped barium hexaferrite nanodiscs. The higher the reaction temperature was, the bigger the as-formed nanodiscs were: (e) 210 °C, (f) 260 °C, (g) 310 °C, and (h) 340 °C (reproduced with permission of the American Chemical Society and Elsevier from refs. [36, 40, 41]).

properties due to size-dependent spin exchange effects, shape is related to switching properties of MNPs due to shape-induced, magnetic anisotropy [34]. If the shape of the MNPs is anisotropic, they may further adopt a certain orientation with respect to the nematic order. Platelet-shaped MNPs, for example, resulted in LC hybrids where an equilibrated interplay between attractive magnetic interactions and LC-mediated repulsive forces induced MNP alignment and ferromagnetic ordering [10]. Effects of nanoparticle shape on transition temperature, order parameter and mobility in LC-based dispersions were further elucidated by Monte Carlo computer simulations [35]. In case of plasmonic Au particles, a remarkable amplification of chirality was recently also achieved for nematic LCs by desymmetrization of spherical nanoparticles to nanorods [26]. The synthesis of monodispersive nanorods (<100 nm) is challenging. In order to break the structural symmetry of, for example, Fe<sub>3</sub>O<sub>4</sub>, polymers or soft, micellar templates have to be used to induce anisotropic nanorod growth. Fe<sub>3</sub>O<sub>4</sub> nanorods  $(27.0 (\pm 9.1) \times 5.5 (\pm 1.0) \text{ nm})$ , for example, have been synthesized *via* chemical transformation of nanorod seeds (Figure 2b) [36]. The nanorod seeds already displayed the desired anisotropic structure but they were composed of a ferri/ferro (oxide-)hydroxide phase and their magnetic properties were rather poor. Fe<sub>3</sub>O<sub>4</sub>/CoFe<sub>2</sub>O<sub>4</sub> nanorods were further obtained by a simple seed-mediated synthesis. Nanorod seeds were exploited here as a platform for both chemical phase change and growth of CoFe<sub>2</sub>O<sub>4</sub> by thermal codecomposition of cobalt(II) and iron(III) acetylacetonate precursors [36].  $Fe_3O_4$  nanocubes (Figure 2c) were obtained by thermal decomposition of  $Fe(acac)_3$  in benzyl ether in the presence of (1,1'-biphenyl)-4-carboxylic acid at 290 °C [37]. The use

n.d.

MNPs	Figure no.	Size (nm)	$M_S$ (A m $^2$ kg $^{-1}$ )	H <sub>C</sub> (298 K) (mT)
Co <sub>0.6</sub> Fe <sub>2.4</sub> O <sub>4</sub>	Figure 2a	7.4 (±0.9)	37.2	0.0
Fe <sub>3</sub> O <sub>4</sub>	Figure 2b	27 (±9.1)	14.4	0.0
Fe <sub>3</sub> O <sub>4</sub>	Figure 2c	28 (±3.0)	62.9	0.0
Fe <sub>3</sub> O <sub>4</sub>	Figure 2d	38 (±5.7)	63.4	0.0
Sc-doped BaFe <sub>12</sub> O <sub>19</sub> (Ba/Sc = 1:1.0)	Figure 2e	37 (±15)	35.5	43
Sc-doped BaFe <sub>12</sub> O <sub>19</sub> (Ba/Sc = 1:1.1)	Figure 2f	52 (±18)	38.5	50
Sc-doped BaFe <sub>12</sub> O <sub>19</sub> (Ba/Sc = 1:0.8)	Figure 2g	59 (±20)	39.2	57

Table 1: Summary of composition, particle sizes and magnetic properties of the magnetic nanoparticles (MNPs) shown in Figure 2.

of 4'-hexyl-(1,1'-biphenyl)-4-carboxylic acid instead yielded Fe<sub>3</sub>O<sub>4</sub> cuboctahedra (Figure 2d).

168 (±193)

n.d.

Figure 2h

Bulk hexaferrites such as BaFe<sub>12</sub>O<sub>19</sub> are very attractive due to their low cost, hard magnetic properties and stability in air [38]. They display a hexagonal crystal structure with closed packed layers of oxygen ions. Trivalent metal cations (Fe<sup>3+</sup>) are located in interstitial sites, while the heavy ions (e. g., Ba<sup>2+</sup>) enter substitutionally the oxygen layers [39]. Particles of scandium-doped barium hexaferrite with disc-like shape were obtained by hydrothermal synthesis. The lateral dimensions of the nanodiscs were dependent on the reaction temperature and increased from 7 (±4) nm (160 °C) over 70 (±38) nm (240 °C) to 168 (±193) nm (340 °C) (Figure 2e-h) while their height was approximately 5 nm [40]. Table 1 summarizes the magnetic properties (saturation magnetization  $(M_s)$  and coercitivity  $(H_s)$ , sizes and composition of MNPs shown in Figure 2.

#### 2.2 LC matrices

Sc-doped BaFe<sub>12</sub>O<sub>19</sub>(Ba/Sc = 1:0.9)

LCs are composed of anisotropic building units (i.e. mesogens) which are spontaneously oriented along a common direction (along the so-called director n). In the simplest case of a nematic LC, these mesogens show only orientational ordering along the director n but no positional order (Figure 1a). LCs are usually further distinguished into two categories, thermotropic and lyotropic LCs. The influence of different particle parameters on the stability of lyotropic hybrid systems has been systematically investigated and is summarized in Ref. [18]. Thermotropic LCs, where the ordering is a function of the temperature, are typically further distinguished according to the shape of their mesogens, e.g. calamitic (rod-like), discotic (disc-like), sanidic (brick-like or lath-like) or bent-core mesogens (Figure 1b). The majority of LCs is formed by calamitic mesogens which are typically composed of a ridged core (e.g. a biphenyl group) and

Figure 3: Structure of calamitic mesogens forming nematic LCs: 4-cyano-4'-pentylbiphenyl (5CB), 4-cyano-4'-octylbiphenyl (8OCB), 4-cyano-4'-n-octyloxybiphenyl (8OCB) and 8 wt% 4-cyano-4"-pentyl-p-terphenyl (5CT), respectively. E7 is a mixture of different mesogens, i. e. 5CB (51 wt%), 7CB (25 wt%), 8OCB (16 wt%) and 5CT (8 wt%).

flexible end groups (e. g. alkyl or alkoxy chains) (Figure 3). A nitrile residue attached to the biphenyl results in a permanent dipole moment enabling directional alignment in the external electric field. 5CB (Figure 3), for example, is a calamitic mesogen forming a nematic LC at ambient temperature ( $T_{\rm CN}=18$  °C;  $T_{\rm NI}=35$  °C). While the single 5CB molecule has a length of 1.9 nm, dimers with a length of approx. 2.5 nm are formed both in the isotropic and nematic phase by partial overlapping of the biphenyl moieties. Also, mixing of different mesogens may further enhance LC properties. For example, E7 contains mainly 5CB (51 wt%), but also 4-cyano-4'-heptylbiphenyl (7CB) (25 wt%), 4-cyano-4'-n-octyloxybiphenyl (8OCB) (16 wt%) and 4-cyano-4"-pentyl-p-terphenyl (5CT) (8 wt%) (Figure 3) [42]. It likewise forms a nematic phase at ambient temperature but its clearing temperature is shifted to higher temperatures ( $T_{\rm NI}=61$  °C).

LCs can be (re)oriented by electric and/or magnetic fields due to the anisotropy of their electric permittivity ( $\varepsilon_a$ ) or diamagnetic susceptibility ( $\chi_a$ ), respectively [43]. The dielectric anisotropy is in the order of unity (e. g.  $\varepsilon_{a,5CB} = 11$ ) and the required voltages are in the order of a few volts [44]. Due to their very low anisotropy of the diamagnetic susceptibility ( $\chi_a \sim 10^{-6} - 10^{-7}$ ), however, LCs are less sensitive to the magnetic field and their realignment may require a large magnetic field strength being in the order of 1 T [45]. Doping of LCs with MNPs enhances their response to the applied magnetic field, an idea which dates back to Brochard and de Gennes [8].

# 2.3 Integration of MNPs in LC matrices

Entropic alignment of mesogens is the origin of the isotropic–nematic transition in an LC. If particles are immersed in a nematic LC, deformations and topological defects arise in the LC in response to the foreign inclusions. One important feature of LC colloidal dispersions is that the elastic distortions of the director and/or the disturbance of the local order parameter in the vicinity of the MNPs in the host LC crystal lead to LC-mediated interactions between the particles immersed in it, while such interactions are absent in usual colloidal dispersions with isotropic host fluids [45]. Therefore, the tendency of MNPs to agglomerate is much stronger in the anisotropic LC phase than in the corresponding isotropic phase. 5CB in the nematic mesophase is shown in Figure 3a. Oleic acid-functionalized  $Fe_3O_4$  MNPs (particle size 10 nm), for

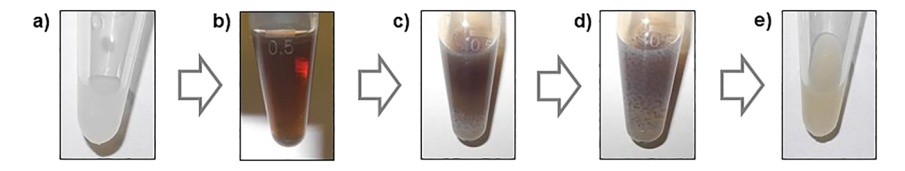


Figure 4: Spontaneous agglomeration of oleic acid-stabilized  $Fe_3O_4$  magnetic nanoparticles (MNPs) (particle size 10 nm) in 5CB during phase transition from the isotropic to the nematic LC phase: (a) 5CB reference; (b) colloidal MNPs in isotropic 5CB host (40 °C; MNP concentration 1 wt%); (c, d) phase transition to the nematic LC phase (<35 °C) where MNP aggregates form; (e) after magnetic separation of the agglomerates, the MNP content in the nematic 5CB host is very low (0.003 wt%), so that the physical properties are hardly affected [33].

example, initially form a homogeneous, colloidally stable dispersion in the isotropic phase of 5CB (40 °C) (Figure 3b) [33]. Under these conditions, they form a ferrofluid which is also stable in the magnetic field. If the temperature is decreased below the clearing temperature of 5CB (<35 °C), the nematic mesophase forms and simultaneously, spontaneous agglomeration of the MNPs occurs (Figure 4c–d). After magnetic separation of the MNP agglomerates, only very low concentrations of MNPs remain in the 5CB LC host (as indicated by the pale light brownish color in Figure 4e) which behaves comparable to undoped 5CB and shows no significant effect in the magnetic field. This is also observed for CoFe<sub>2</sub>O<sub>4</sub> MNPs stabilized by conventional organic acids (such as caproic acid, lauric acid, myristic acid, palmitic acid or oleic acid) even if their particle size is only 2.5–3 nm [33]. Thus, surfactants typically employed for preparing conventional ferrofluids in isotropic hosts are not well-suited to colloidally stabilize MNPs in higher concentrations in anisotropic LC hosts such as 5CB. Indeed, ferronemates described in the literature are usually characterized by limited colloidal stability and very low concentrations of MNPs [91, 46].

The stability of MNP dispersions is typically low and formation of aggregates often occurs even in colloids with low MNP content. In general, the size, shape, topology as well as magnetic and surface properties of the MNPs influence the interactions between MNPs inserted into a medium that is partially ordered, such as a nematic LC [47]. Coagulation of the immersed MNPs is caused by LC-mediated, van der Waals and/or magnetic dipole–dipole interactions which may lead to subsequent phase separation by gravitational forces or magnetic field gradients. The origin of this instability depends on the particle size [24, 25c, 48]: For relatively large particles ( $r_{\rm part}$  > 100 nm), the director  $\boldsymbol{n}$  of the LC is distorted around the particles which gives rise to topological defects and strong attractive orientational elastic interactions between the particles, encouraging MNP aggregation. The elastic distortions of the host LC arise from the anchoring of the mesogens on the particle surface. The force of these interactions has a strong topological signature [47]. For small particles ( $r_{\rm part}$   $\ll$  100 nm), distortion of the LC director is not favored energetically resulting in a macroscopically uniform

alignment and thus, orientational elastic forces do not contribute significantly to the aggregation process. In this case, interactions due to disturbance of the local order parameter *S* of the LC in the vicinity of the nanoparticles might play an important role [25b]. However, since the behavior of MNPs immersed in an LC is more complex and not only influenced by particle size alone, the transition between these two size regimes may be fluent. In order to prevent aggregation of the MNPs and phase separation, the surface of the MNPs must therefore be considered at the molecular level and the particle-matrix interaction must be specifically tailored by use of suitable ligands.

#### 2.3.1 Synthesis of long-chain, (pro)mesogenic ligands

General concepts for stabilization of MNPs in conventional isotropic hosts can't be simply transferred to LC hosts. In ferrofluids, for example, the surface of the MNP surface is typically coated by conventional surfactants (such as oleic acid) to increase the (electro)steric repulsion radius and thus kinetically stabilize the MNPs in the isotropic host. In the case of nematic LC hosts, however, the interaction of the surfactants with the MNP surface and the LC host needs to be specifically tailored in such a way that the disturbance of the LC order in the proximity of the particles is minimized as much as possible. This may be achieved by use of (pro)mesogenic ligands. The role of these (pro)mesogenic ligands is not only steric repulsion by a large exclusion volume, but also to smooth out the disturbance of the local LC director at the MNP-LC interface [25c]. (Pro)mesogenic ligands are typically composed of three structural parts: (1) a functional group that allows for binding to the respective MNPs which is linked by (2) a flexible spacer to (3) the (pro)mesogenic structural unit.

A series of long-chain, (pro)mesogenic ligands (1–8) was synthesized in which the (pro)mesogenic structural unit was either cyanobiphenyl or octylbiphenyl. This (pro) mesogenic unit was linked via an alkyl chain of different lengths ( $-(CH_2)_n$ – with n = 6, 7, 14, 15, 16, 17, or 25) to a functional group for nanoparticle binding (a carboxylate, phosphate or amino group) (Figure 5) [21]. Ligands 1–3 were obtained with a yield of

Figure 5: Synthesis of the long-chain, aliphatic, (pro)mesogenic ligands 1-8 [21, 49].

76–79% *via* etherification. A Gabriel reaction with an imide, followed by deprotection, gave the amine-functionalized ligand **4**. The organophosphate ligand **5** was received in a yield of 47%. For n = 17 and 25, a modified Negishi coupling was employed to yield the ligands **6** and **7**. The corresponding carbonic acids, however, were insoluble in common organic solvents and thus, only **6** has been deprotected and used without further characterization for the coating of MNPs [49]. Ligand **8** was synthesized in a three-step procedure using (1) a Sonogashira cross-coupling, (2) followed by a Pd-catalyzed reduction of the triple bond with hydrogen and (3) an etherification [49].

#### 2.3.2 Synthesis of dendritic, (pro)mesogenic ligands

The tendency of MNPs to aggregate in LC hosts can be considerably reduced by use of long-chain (pro)mesogenic ligands enabling the preparation of homogeneous, colloidal dispersions of very small MNP in 5CB (see below). If the MNPs are immersed in the nematic LC, however, the mutual molecular alignment not only disturbs the local order of the LCs in the vicinity of the MNPs, but also the originally isotropic, spherical ligand shell at the MNP surface (Figure 5a). The (pro)mesogenic ligands get aligned parallel to the local director field leading to an increased ligand density at the MNP poles and to their equatorial depletion. The distortion of the ligand shell from spherical to tactoidal further encourages MNP agglomeration (Figure 6b) [25b]. In general, however, the process of agglomeration in these systems seems to be more complex.

(Pro)mesogenic ligands with dendritic structure reduce the distortion of the ligand shell and prevent equatorial ligand depletion, thus minimizing the tendency for MNP agglomeration [22, 25c]. However, the preparation of these (pro)mesogenic dendritic ligands typically requires multistep synthetic procedures which yield only small amounts of the target ligands [50]. In this context, we developed a convergent synthetic procedure for different ligands with mesogenic structural units and dendritic structure

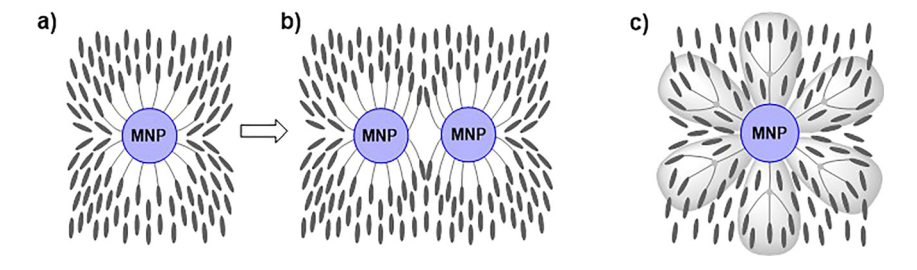


**Figure 6:** Simplified, schematic representation of ligand-functionalized MNPs in 5CB: (a) The alignment of (pro)mesogenic ligands at the MNP surface induces a tactoidal morphology with increased ligand density at the particle poles and equatorial depletion, which (b) favors the formation of MNP clusters. In general, however, the overall agglomeration process in these systems seems to be complex. (c) Dendritic-ligand-functionalized MNPs further increase the exclusion volume leading to an increased stability in 5CB.

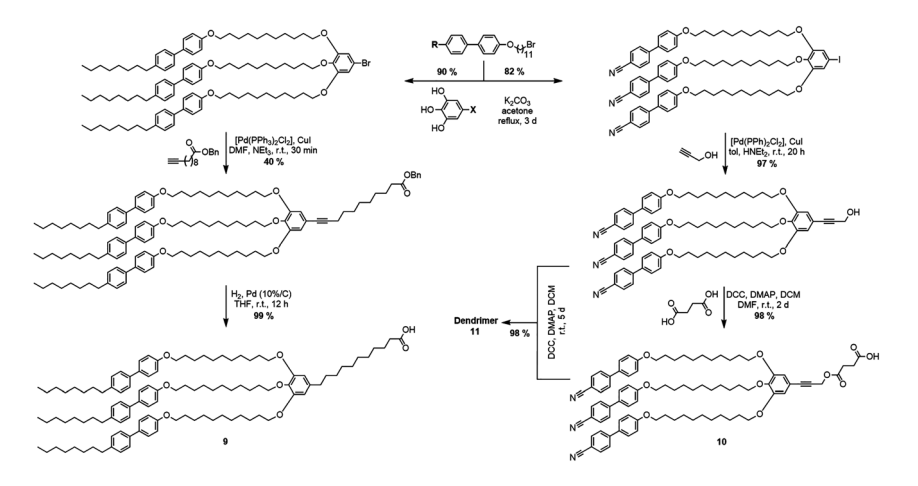


**Figure 7:** Synthetic procedure for different dendritic ligands with mesogenic structural units. In general, this strategy may be exploited for further tailoring the structure of dendritic ligands (e.g. in terms of spacer length, MNP binding group and (pro)mesogenic structural unit) or to obtain also dendrimers as shown for **11** [49].

(Figure 7) [49]. A three-step sequence of etherification, Sonogashira cross-coupling and esterification or deprotection the (pro)mesogenic dendritic ligands in overall good yields. Starting from literature known 5-iodobenzene-1,2,3-triol, for example, yielded the dendritic ligand **10** with an overall yield of 77 %. Since this procedure is highly versatile, it could be further extended to dendritic ligands with different spacer lengths and MNP binding groups, e.g. **11** (Figure 7). In preliminary experiments, electrostatically stabilized MNPs with larger diameter were coated by these dendritic ligands and stabilized in the nematic phase of 5CB. These experiments are very promising with regard to the future stabilization of larger (anisotropic) MNPs.

In order to get insights into the temperature-dependent, LC behavior of the dendritic ligands **10** and dendrimer **11**, we investigated both compounds via POM. For **10**, a mesophase was formed but it was stable only in a small temperature range ( $\Delta T = 0.2$  °C): The transition from the isotropic to the smectic A-phase took place at  $T_{\rm SmA~I} = 88.2$  °C (Figure 8a), while the crystalline phase was formed at  $T_{\rm Cr~SmA} = 88.0$  °C. The characteristic, fan-shaped textures of the smectic A-phase was also observed for dendrimer **11**, but the textures were much more pronounced (Figure 8b) [51]. In case of dendrimer **11**, the transition from the isotropic to the smectic A-phase occurred at  $T_{\rm SmA~I} = 104.9$  °C and at  $T_{\rm SmC~SmA} = 98$  °C a smectic C-phase was formed (Figure 8c). In addition to the fanshaped textures, star-like defects were observed [51]. The smectic C-phase was maintained down to  $T_{\rm Cr~SmC} = 86$  °C.



**Figure 8:** Polarizing microscopy (POM) images (under crossed polarizers) of dendritic ligand **10** and dendrimer **11:** The samples (a) **10** and (b) dendrimer **11** were placed between glass slides and show the characteristic, fan-shaped texture of a smectic A-phase. (c) The POM image of dendrimer **11** in an LC test cell (10  $\mu$ m; planar cell rubbing) shows the characteristic texture of the smectic C-phase (Characteristic phase transition temperatures: **10:**  $T_{\text{SmA I}} = 88.2 \,^{\circ}\text{C}$ ,  $T_{\text{Cr SmA}} = 88.0 \,^{\circ}\text{C}$ ; dendrimer **11:**  $T_{\text{Cr SmC}} = 86 \,^{\circ}\text{C}$ ,  $T_{\text{SmC SmA}} = 98 \,^{\circ}\text{C}$ ,  $T_{\text{SmA I}} = 104.9 \,^{\circ}\text{C}$ ) [41].

#### 2.3.3 Coating of magnetic nanoparticles with (pro)mesogenic ligands

The absence of strongly coordinating ligands in case of electrostatically stabilized MNPs facilitates post-synthetic surface engineering of the MNPs. Electrostatically stabilized MNPs (e. g.  $Fe_3O_4$ ,  $CoFe_2O_4$ ,  $CuFe_2O_4$ ,  $NiFe_2O_4$ ,  $ZnFe_2O_4$ ) with very small particle sizes

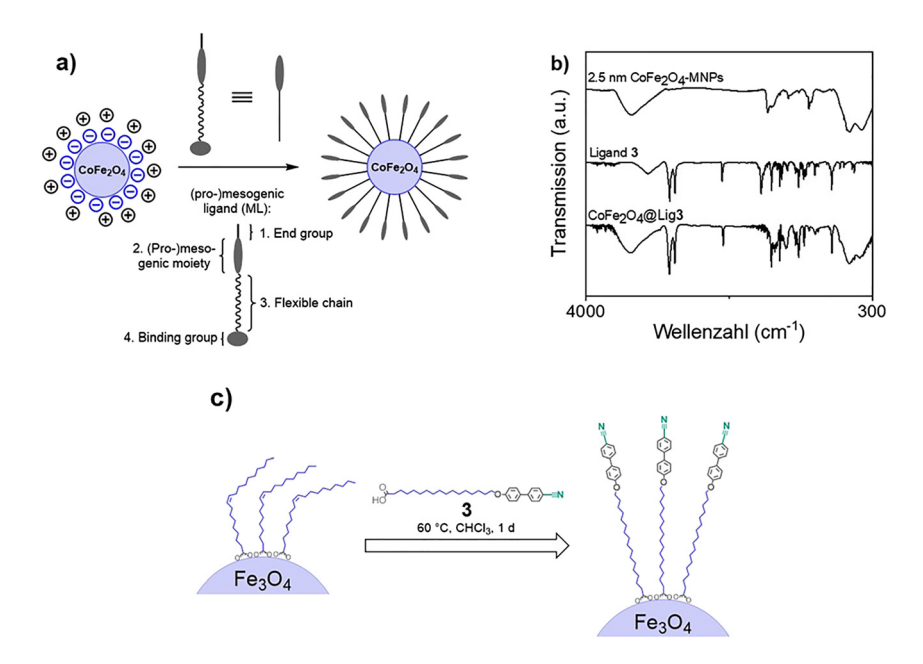


**Figure 9:** Functionalization of CoFe<sub>2</sub>O<sub>4</sub> MNPs with conventional aliphatic and (pro)mesogenic ligands: (a) Schematic representation of the approach followed to generate functionalized MNPs. (b) Comparison of IR spectra confirmed a successful functionalization with (pro)mesogenic ligand **3** of CoFe<sub>2</sub>O<sub>4</sub> MNPs. (c) Ligand exchange-based approach was exploited to functionalize different MNPs, e. g. 5.3 nm Fe<sub>3</sub>O<sub>4</sub>@oleate MNPs to yield 5.3 nm Fe<sub>3</sub>O<sub>4</sub>@Lig**3**-MNPs. The exchange reaction and the purity of the as-synthesized MNPs was verified *via* IR spectroscopy.

were functionalized and purified modularly with the (pro)mesogenic ligands using a process developed by us (Figure 9a) [21, 33]. DMF was used in the coating procedure as a solvent for the electrostatically stabilized MNPs and the (pro)mesogenic ligands. The MNPs coated with ligands were then thoroughly purified by repeated magnetic separation. IR spectra demonstrate the successful functionalization of the MNPs and the attachment of the ligands to the particle surface (Figure 9b). The amount of ligand loading on the MNP surface was determined by thermogravimetry (TGA). The saturation magnetization of the particles was small due to the small particle size and the large surface-to-volume ratio. Spin canting at the MNP surface, crystal defects or formation of a nonmagnetic dead layer usually lead to lower saturation magnetizations in MNPs compared to bulk material.  $M_{1T}$  (298 K) of the 2.5 nm size, ligand coated MNPs was in the range of 2.4–5.5 A m<sup>2</sup> kg<sup>-1</sup> depending on the type of ligand coating (in some cases, no saturation was reached for the applied magnetic field (1 T)).

Thermal decomposition of metal precursors, e.g., at high reaction temperatures in the presence of strongly coordinating ligands yields MNPs of high crystallinity and often, enhanced magnetic properties. In general, these ligands control nucleation and growth processes in the synthetic procedure and they stabilize the as-formed MNPs. Any change to this reaction parameter will critically influence the quality of the final MNPs. Therefore, in case of MNPs where the synthesis required the presence of strongly coordinating ligands, another strategy had to be pursued to functionalize the MNPs by (pro)mesogenic ligands. In this case, the (pro)mesogenic ligands were introduced *via* post-synthetic ligand exchange (Figure 9c). This ligand exchange reaction critically depends on various reaction parameters (e. g. binding group, solubility and size of MNPs) and needs to be optimized for every MNP-(pro)mesogenic ligand system. Chloroform at 60 °C, for example, turned out to be a suitable medium to functionalize 5.3 nm, oleic acid-stabilized Fe<sub>3</sub>O<sub>4</sub> MNPs with the (pro)mesogenic ligand 3 (corresponding IR spectrum is not shown here). Purification of the MNP functionalized with (pro)mesogenic ligands is important and none of the conventional ligand used for previous MNP synthesis and also no free (pro)mesogenic ligands should remain in the sample.

#### 2.3.4 Influence of the structure of the (pro)mesogenic ligands on the interaction of the MNPs with the LC host

The MNPs which were coated with (pro)mesogenic ligands were then integrated in the LC host. After ultrasonic treatment, 2.5 nm sized CoFe<sub>2</sub>O<sub>4</sub> MNPs coated with (pro) mesogenic ligands, for example, formed a colloidal dispersion in the isotropic phase of 5CB (Figure 10b). During the transition to the nematic 5CB phase, some macroscopic agglomerates were formed, which could be easily separated with a laboratory magnet (Figure 10c,d). A brown-colored, colloidal MNP dispersion was obtained in the nematic 5CB phase, which was stable in a magnetic field gradient (laboratory magnet) and also showed long-term colloidal stability in the LC host (>5 months) (Figure 10e). No macroscopic agglomerates were observed under crossed polarizers. For CoFe<sub>2</sub>O<sub>4</sub> MNPs coated with  $3 (M_{1T} (298 \text{ K}) = 5.5 \text{ A} \text{ m}^2 \text{kg}^{-1})$ , for example, a colloidally stable CoFe<sub>2</sub>O<sub>4</sub>-5CB hybrid material with a concentration of 0.12 wt% could be synthesized. More details on magnetic properties and magnetization curves of CoFe<sub>2</sub>O<sub>4</sub> MNPs coated with 3 are reported in refs. [21, 33]. While the undoped 5CB exhibited the usual diamagnetic behavior with identical magnetization curves in the nematic and isotropic phases, the magnetic CoFe<sub>2</sub>O<sub>4</sub>-5CB hybrid (0.085 wt%) behaved as a superparamagnet at low magnetic field (displaying no hysteresis) with a sharp knee in the magnetization curve [23]. Due to interaction between mesogens and MNPs via ligands, the change of the mesogen orientation also reorients the MNPs, a behavior observed as a sharp knee in the magnetization curve. No significant increase of the clearing temperature  $T_{N-1}$  (0.5 °C via differential scanning calorimetry (DSC) was observed after doping 5CB with MNPs. The structure of the (pro)mesogenic ligands was highly important and influenced the MNP content of the final colloidal MNP dispersion in the LC host. We could show, for example, that carboxylate binding groups were suitable for binding of (pro)mesogenic ligands to the surface of e. g. CoFe<sub>2</sub>O<sub>4</sub> MNPs. Ligand loadings of up to 50 wt% were achieved for CoFe<sub>2</sub>O<sub>4</sub> MNPs using ligand **3** [33]. If the size of the **3**-coated CoFe<sub>2</sub>O<sub>4</sub> MNPs was slightly increased from 2.5 nm over 3.0 -4.4 nm, the MNP concentration decreased from 0.12 wt% over 0.08 to 0.04 wt%, respectively. It is important to note here, that only MNPs were considered that remained colloidally stable and dispersed in the nematic phase of the 5CB host after exposure to a magnetic field gradient. As shown in Figure 10f, the length of the flexible linker  $(-(CH_2)_n-)$  also influenced the effective

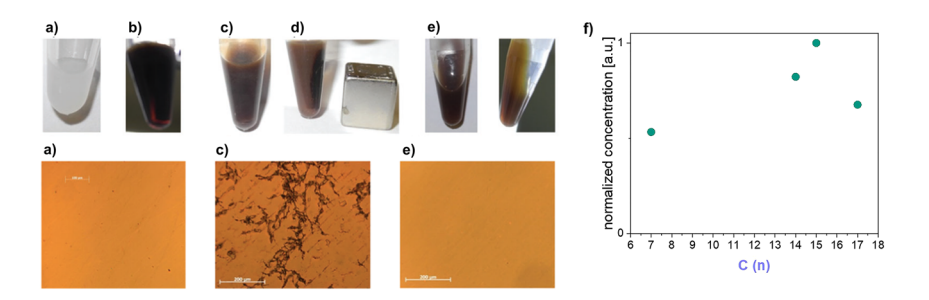


Figure 10: Integration of 2.5 nm size CoFe<sub>2</sub>O<sub>4</sub> MNPs coated with (pro)mesogenic ligand 3 in 5CB: (a) 5CB, (b) colloidal MNP dispersion in the isotropic 5CB phase, (c) after transition to the nematic 5CB phase, (d) magnetic separation of macroscopic agglomerate and (e) stable colloidal MNP dispersion (0.12 wt%) in the nematic phase of 5CB. The corresponding POM images (under crossed polarizers) of the thin film samples in a LC test cell (25 µm, parallel cell rubbing) are shown below (Reproduced from Ref. [20] with permission from the Physical Chemistry Chemical Physics Owner Societies). (f) The concentration of MNPs (mass fraction of cobalt ferrite as determined by inductively coupled plasma optical emission spectroscopy (ICP-OES)) in their stable colloidal dispersion in the nematic 5CB phase depends on the chain lengths of the (pro)mesogenic ligand [41].

particle concentration in the stable colloidal MNP dispersion after magnetic separation (n = 7, 14, 15, 17 for 1, 2, 3 and 6, respectively).

For CoFe<sub>2</sub>O<sub>4</sub> MNPs, the particle content of the 5CB LC increased with the chain length of the linker (Figure 10f). However, it seemed to reach a maximum for n = 15 and further increase of the alkyl chain length to n = 17 did not allow for stabilizing higher MNP concentrations in the 5CB LC. As the length of the alkyl chain increases, the flexibility of the (pro)mesogenic units of the ligands on the MNP surface is improved. This does not only increase the steric MNP repulsion by a larger exclusion volume but also seemed to effectively smooth out the disturbance of the LC in the vicinity of the MNPs. However, the longer the ligands get, the less they resemble also the structure of 5CB which counteracts the stabilization by the bigger exclusion volume. Moreover, the structure of the mesogenic unit influences the MNP stability in the nematic phase of 5CB. MNPs functionalized by (pro)mesogenic ligands with either octylbiphenyl (8) or cyanobiphenyl group (3) and otherwise similar structure showed a significantly different behavior when immersed in 5CB (Figure 11). No MNPs remained in the 5CB LC

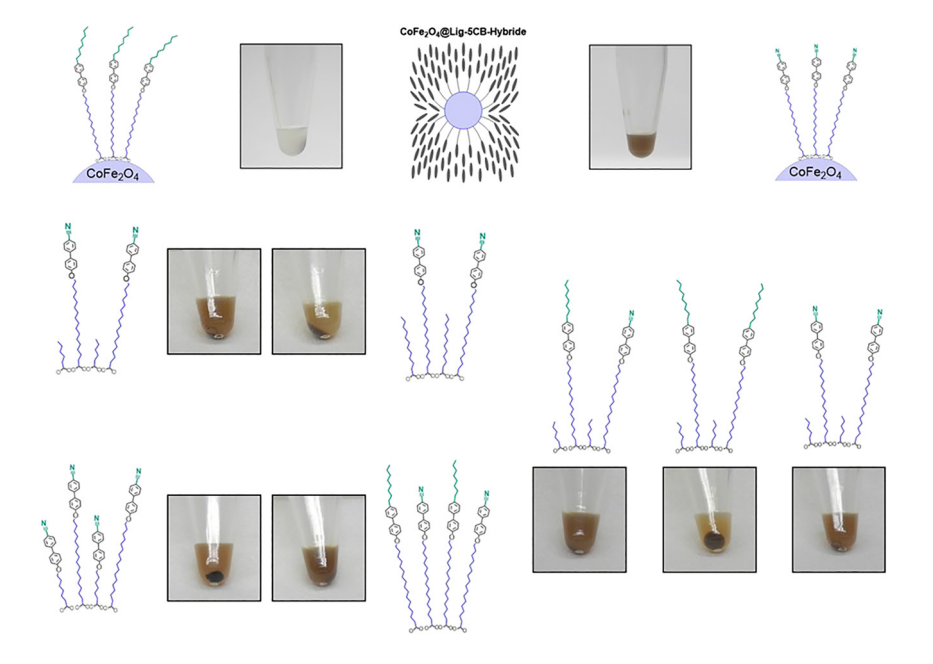


Figure 11: Influence of the end group on the stability: schematic representation and photograph, respectively, of the hybrids. The comparison of (pro)mesogenic ligands with different group on the biphenyl moiety shows that ligands with nitrile groups stabilizes the MNPs more efficiently in 5CB. Here, also the influence of coligands (caproic acid, lauric acid) and mixed (pro)mesogenic ligands (ML1/ML3; ML3/ML8) on the colloidal stability of the MNPs in 5CB is shown. This illustrates the importance of MNP-matrix interactions in these systems and the need for a highly specific surface engineering of the MNPs [41].

after magnetic separation of the **8**-coated MNPs, while the brown color of the sample indicates the successful stabilization of the MNPs coated by **3**. Interestingly, if the MNPs were coated with a mixture of both ligands **3** and **8** (Figure 11), even higher MNP concentrations were achieved.

The additional use of smaller co-ligands was reported to allow for increasing and optimizing the contact area between the LC mesogens and the mesogenic structural units on the surface of the MNPs [25a, 25c]. They also increase the angle-dependent mobility of the (pro)mesogenic ligand, enabling their optimized alignment with respect to the 5CB host. Both the molar ratio of the (pro)mesogenic ligand/coligand and their relative lengths play a role here. In a systematic series of experiments, the influence of different coligands (caproic acid, lauric acid) and molar ratios (1:1; 1:2) on the stability of MNPs in 5CB was investigated (Figure 11). In these experiments, however, it turned out that the correlation between the functionalized surface and the stability in 5CB is complex.

#### 2.4 Characterization of MNPs in LC hosts

The magneto-optical properties of the MNP-5CB hybrids were investigated in electric ( $n \perp E$ ), magnetic ( $n \perp B$ ) and combined fields ( $n \parallel B \perp E$  and  $n \perp B \parallel E$ ) in collaboration with R. Stannarius and A. Eremin [21]. The Fréedericksz transition in the electric and/or magnetic field was investigated by capacitance and optical measurements of the 2.5 nm size  $CoFe_2O_4$  MNPs coated by linear, (pro)mesogenic ligands (1, 3, 4, 5) in commercial LC test cells. For MNPs with different linear, (pro)mesogenic ligands (1, 3, 4, 5) and different concentrations in 5CB (0.03-0.12 wt%), the electrical Fréedericksz transition was not significantly affected by the embedding of the MNPs in the LC. Also the birefringence of the MNP-5CB hybrids was the same as for pure 5CB. A decrease of the threshold for the magnetic Fréedericksz transition, however, was observed in the external magnetic field. For MNPs with the same particle size (2.5 nm) and different ligands (1, 3, 4, 5), the magnetic Fréedericksz threshold 2.5 nm and different ligands (3.5 nm), the magnetic Fréedericksz threshold 3.5 nm and different ligands (3.5 nm), the magnetic Fréedericksz threshold 3.5 nm and different ligands (3.5 nm), the magnetic Fréedericksz threshold 3.5 nm and different ligands (3.5 nm), the magnetic Fréedericksz threshold 3.5 nm and different ligands (3.5 nm), the magnetic Fréedericksz threshold 3.5 nm and different ligands (3.5 nm), the magnetic Fréedericksz threshold 3.5 nm and different ligands (3.5 nm), the magnetic Fréedericksz threshold 3.5 nm and different ligands (3.5 nm), the magnetic Fréedericksz threshold 3.5 nm and different ligands (3.5 nm), the magnetic Fréedericksz threshold 3.5 nm and different ligands (3.5 nm).

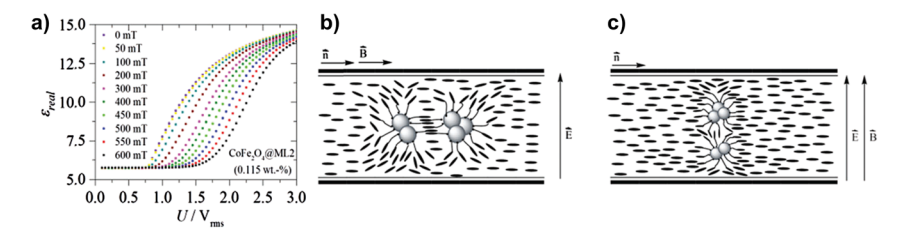
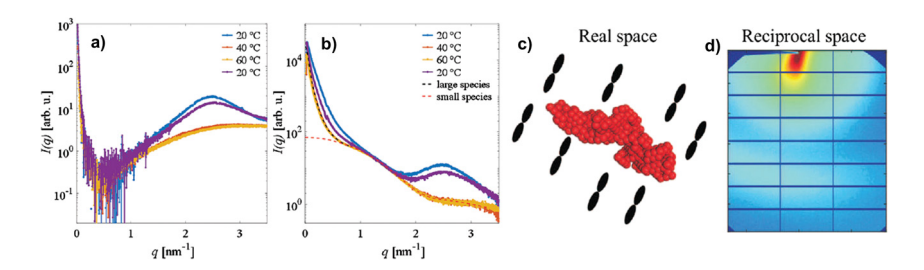


Figure 12: Electro- and magneto-optical effects of  $CoFe_2O_4$  MNPs coated with a linear, (pro) mesogenic ligand (3): (a) Dependence of the electric threshold on the magnetic induction  $\boldsymbol{B}$  for crossed fields ( $\boldsymbol{n} \parallel \boldsymbol{B} \perp \boldsymbol{E}$ ). Cartoon illustrating the potential behavior of anisotropic MNP aggregates in (b) crossed ( $\boldsymbol{n} \parallel \boldsymbol{B} \perp \boldsymbol{E}$ ) and (c) parallel ( $\boldsymbol{n} \perp \boldsymbol{B} \parallel \boldsymbol{E}$ ) fields (Reproduced from Ref. [21] with permission from the PCCP Owner Societies).



**Figure 13:** Temperature-dependent SAXS intensity of (a) the 5CB reference and (b) 3 nm sized, **3**-coated  $CoFe_2O_4$  MNPs in 5CB. (c) *Ab initio* model showing aggregate orientation with respect to the 5CB dimers. (d) 2D SAXS pattern at T = 20 °C (reproduced with permission of the Royal Society of Chemistry from ref. [23]).

concentration in 5CB. This indicated that the magnetic properties of the MNPs and their interaction with the 5CB host were responsible for the observed shifts. The electrical Fréederick transition was also investigated under a bias magnetic field either parallel ( $n \perp B \parallel E$ ) or perpendicular ( $n \parallel B \perp E$ ) to the applied electric field. In this case, the alignment of the director n of the LC host lead either to an increase ( $n \parallel B \perp E$ ) or decrease ( $n \perp B \parallel E$ ) of the electric threshold field. If the magnetic field was perpendicular to the electric field ( $n \parallel B \perp E$ ), the MNPs seemed to counteract the influence of the external magnetic field on the alignment of the 5CB mesogens (Figure 12a). Based on the Burylov-Raikher theory, the formation of anisotropically-shaped MNP clusters in the 5CB was suggested to explain this counterintuitive behavior (Figure 12b,c). Due to the small size of the MNPs, formation of the anisotropic aggregates should not be induced by magnetic dipole interaction but rather by interaction of the MNPs with the surrounding LC host.

Based on these results, the interaction of the LC with the MNPs was further investigated by small-angle X-ray scattering (SAXS) and by a superconducting quantum interference device magnetometer (SQUID) [23] In SAXS measurements of 3 nm sized, 3-coated CoFe<sub>2</sub>O<sub>4</sub> MNPs in 5CB, a strong signal was observed for MNPs at smaller scattering vectors  $\mathbf{q}$  besides the scattering contribution of 5CB (Figure 13). Interestingly, this signal was anisotropic and pointed to the direction of the LC nematic director n. If the LC was heated above the clearing point  $T_{\rm NI}$  (40 °C), where it forms the isotropic phase, the SAXS patterns became also isotropic. If the sample was cooled below  $T_{NI}$ , the SAXS pattern became anisotropic again, but to a lesser extent. Refinement of the SAXS data yielded a mean size of the MNPs of 3.8 nm, which was in good agreement with the results of the analysis of the MNPs by TEM and dynamic light scattering. However, the characteristic shape of the pair-distance distribution function and the anisotropic scattering pattern in the nematic 5CB phase also strongly pointed to the formation of small, anisotropicallystructured MNP aggregates (with a long axis of approximately 100 nm). Overall, the 5CB LC was well oriented with the long axis of the MNP clusters oriented perpendicular to the 5CB long axis (Figure 13). Magnetic measurements of the MNPs in 5CB revealed the typical behavior of a superparamagnetic system up to a field strength of approximately 557 kA m<sup>-1</sup> where the magnetic order seemed to change. As the magnetic field strength was further increased, only the diamagnetic contribution from 5CB was observed.

### 3 Conclusion and outlook

Hybridization of MNPs and LCs can effectively modify the electro- and magneto-optic responses and other physical characteristics of the LCs. The MNP-matrix interactions in these systems, however, are highly complex and depend on various parameters related to the size, shape, topology, surface structure and magnetic properties of the MNPs on one side and the structure and dimensions of the LC mesogens on the other side. Elastic distortions of the host LC crystal can mediate attractive interactions between the MNPs, while such interactions are absent in usual colloidal dispersions with isotropic ferrofluids. Therefore, the tendency of MNPs to agglomerate is much stronger in the anisotropic LC phase than in the corresponding isotropic phase. Surface engineering of MNPs using tailored (pro)mesogenic ligands can tackle this challenge. In this context, a library of different (pro)mesogenic ligands has been established where the structural parts (i. e., MNP binding group, spacer length of alkyl chain and mesogenic unit) were systematically addressed and varied. The structure of the (pro)mesogenic ligands critically influences the MNP-matrix interactions and the stability of the colloidal MNP dispersion in the LC host. The increase in spacer length to up to 15 C atoms increased the overall MNP stability in 5CB, while its further increase decreased stability. Moreover, the structure of the mesogenic unit was highly important and a nitrile group was shown to be beneficial for MNP stabilization. Small MNPs were functionalized by these (pro)mesogenic ligands and stabilized in the nematic phase of 5CB. The doping of 5CB LC with these MNPs leads to a decrease of the magnetic Fréedericksz transition threshold. As shown by SAXS measurements, the MNPs formed anisotropic structures in 5CB which lead to an interesting behavior particularly in crossed electric and magnetic fields. However, with these ligands the stabilization in 5CB was restricted to small MNP sizes. If the particle size was further increased, colloidal dispersions of lower MNP content were achieved. In this context, sterically more demanding, (pro)mesogenic ligands with dendritic structures might be highly interesting. This may enable the functionalization of larger (anisotropic) MNPs and their successive stabilization in 5CB, where interesting effects on the magnetooptical properties may be expected.

The contactless nature of magnetic manipulation and versatility of magnetic, magneto-optical and magneto-electro-optical effects are extremely attractive for various applications (e. g. in LCDs or sensors). In this context, further enhancement of the sensitivity to the magnetic field and decrease of the magnetic Fréedericksz threshold may be achieved by long-term colloidal stabilization of larger MNPs with improved magnetic properties (e. g. higher  $M_s$ ). In addition, the stabilization of MNPs with anisotropic shape (such as nanorods) may further enhance the switching properties. Here, also the modulation of the LC structure (e. g. in terms of chirality) is

certainly another very interesting aspect. Moreover, LC-mediated assembly of nanoparticles has recently attracted a lot of interest. It may not only lead to LCs with ferromagnetic properties but also to novel and complex, nanoparticle-based superstructures. The parameter space is large here which opens up many possibilities for future studies on active matter and programmable liquid constructs.

**Author contribution:** All the authors have accepted responsibility for the entire content of this submitted manuscript and approved submission.

Research funding: This work was supported by Deutsche Forschungsgemeinschaft (BE 2243/2-1, BE 2243/2-2, BE 2243/2-3).

**Conflict of interest statement:** The authors declare no conflicts of interest regarding this article.

### References

- 1. a) Shen Y, Dierking I. Perspectives in liquid-crystal-aided nanotechnology and nanoscience. Appl Sci 2019;9:2512-59. b) Chernyshuk SB, Lev BI, Yokoyama H. Paranematic interaction between nanoparticles of ordinary shape. Phys Rev E 2005;71:062701-1-4.
- 2. Qi H, Hegmann T. Impact of nanoscale particles and carbon nanotubes on current and future generations of liquid crystal displays. J Mater Chem 2008;18:3288-94.
- 3. Hu W, Zhao H, Shan L, Song L, Cao H, Yang Z, et al Magnetite nanoparticles/chiral nematic liquid crystal composites with magnetically addressable and magnetically erasable characteristics. Liq Cryst 2010;37:563-9.
- 4. Rupnik PM, Lisjak D, Čopič M, Mertelj A. Ferromagnetic liquid crystals for magnetic field visualisation. Liq Cryst 2015;42:1684-8.
- 5. a) Zadoina L, Lonetti B, Soulantica K, Mingotaud AF, Respaud M, Chaudret B, et al Liquid crystalline magnetic materials. J Mater Chem 2009;19:8075-8. b) Riou O, Lonetti B, Davidson P, Tan RP, Cormary B, Mingotaud A-F, et al Liquid crystalline polymer-co nanorod hybrids: structural analysis and response to a magnetic field. J Phys Chem B 2014;118:3218-25. c) Riou O, Lonetti B, Tan RP, Harmel J, Soulantica K, Davidson P, et al Room-temperature, strain-tunable orientation of magnetization in a hybrid ferromagnetic co nanorod-liquid crystalline elastomer nanocomposite. Angew Chem Int Ed 2015;54:10811-15. d) Kaiser A, Winkler M, Krause S, Finkelmann H, Schmidt AM. Magnetoactive liquid crystal elastomer nanocomposites. J Mater Chem 2009;19:538-43. e) Garcia-Márquez A, Demortière A, Heinrich B, Guillon D, Bégin-Colin S, Donnio B. Iron oxide nanoparticle-containing main-chain liquid crystalline elastomer: towards soft magnetoactive networks. J Mater Chem 2011;21:8994-6.
- 6. Song HM, Kim JC, Hong JH, Lee YB, Choi J, Lee JI, et al Magnetic and transparent composites by linking liquid crystals to ferrite nanoparticles through covalent networks. Adv Funct Mater 2007;17:2070-6.
- 7. a) Fleischmann E-K, Zentel R. Liquid-crystalline ordering as a concept in materials science: from semiconductors to stimuli-responsive devices. Angew Chem Int Ed 2013;52:8810-27. b) Tschierske C. Development of structural complexity by liquid-crystal self-assembly. Angew Chem Int Ed 2013; 52:8828–78. c) Bisoyi HK, Li Q. Light-driven liquid crystalline materials: from photo-induced phase transitions and property modulations to applications. Chem Rev 2016;116:15089-166.
- 8. Brochard F, de Gennes PG. Swelling equilibrium and light spectroscopy in swollen polymeric networks at theta conditions. J Phys (France) 1970;31:691-708.

- 9. a) Chen S-H, Amer NM. Observation of macroscopic collective behavior and new texture in magnetically doped liquid crystals. Phys Rev Lett 1983;51:2298-301. b) Bacri JC, Neto AMF. Dynamics of lyotropic ferronematic liquid crystals submitted to magnetic fields. Phys Rev E 1994; 50:3860-4. c) Ponsinet V, Fabre P, Veyssié M. Transition of a ferrosmectic in a very weak magnetic field. Europhys Lett 1995;30:277-82. d) Berejnov V, Cabuil V, Perzynski R, Raikher Y. Lyotropic system potassium laurate/1-decanol/water as a carrier medium for a ferronematic liquid crystal: phase diagram study. J Phys Chem B 1998;102:7132-8. e) Berejnov V, Raikher Y, Cabuil V, Bacri JC, Perzynski R. Synthesis of stable lyotropic ferronematics with high magnetic content. J Colloid Interface Sci 1998;199;215-7. f) Berejnov V, Bacri JC, Cabuil V, Perzynski R, Raikher Y. Lyotropic ferronematics: magnetic orientational transition in the discotic phase. Europhys Lett 1998;41: 507-12. g) Ramos L, Fabre P, Fruchter L. Magnetic field induced instabilities of a doped lyotropic hexagonal phase. Eur Phys J B 1999;8:67-72. h) Cruz CD, Sandre O, Cabuil V. Phase behavior of nanoparticles in a thermotropic liquid crystal, I Phys Chem B 2005;109;14292-9, i) Buluy O. Nepijko S, Reshetnyak V, Ouskova E, Zadorozhnii V, Leonhardt A, et al Magnetic sensitivity of a dispersion of aggregated ferromagnetic carbon nanotubes in liquid crystals. Soft Matter 2011;7: 644-9. j) Vallooran JJ, Bolisetty S, Mezzenga R. Macroscopic alignment of lyotropic liquid crystals using magnetic nanoparticles. Adv Mater 2011;23:3932-7. k) Kopčanský P, Tomašovičová N, Koneracká M, Timko M, Závišová V, Džarová A, et al Phase transitions in liquid crystal doped with magnetic particles of different shapes. Int J Thermophys 2011;32:807-17. l) Podoliak N, Buchnev O, Bavykin DV, Kulak AN, Kaczmarek M, Sluckin TJ. Magnetite nanorod thermotropic liquid crystal colloids: synthesis, optics and theory. J Colloid Interface Sci 2012;386:158-66. m) Garbovskiy Y, Baptist JR, Thompson J, Hunter T, Lim JH, Min SG, et al Increasing the switching speed of liquid crystal devices with magnetic nanorods. Appl Phys Lett 2012;101:181109-1-5.
- 10. Mertelj A, Lisjak D, Drofenik M, Čopič M. Ferromagnetism in suspensions of magnetic platelets in liquid crystal. Nature 2013;504:237-41.
- 11. Shuai M, Klittnick A, Shen Y, Smith GP, Tuchband MR, Zhu C, et al Spontaneous liquid crystal and ferromagnetic ordering of colloidal magnetic nanoplates. Nat Commun 2016;7:10394.
- 12. Mertelj A, Osterman N, Lisjak D, Čopič M. Magneto-optic and converse magnetoelectric effects in a ferromagnetic liquid crystal. Soft Matter 2014;10:9065-72.
- 13. a) May K, Eremin A, Stannarius R, Peroukidis SD, Klapp SHL, Klein S. Colloidal suspensions of rodlike nanocrystals and magnetic spheres under an external magnetic stimulus: experiment and molecular dynamics simulation. Langmuir 2016;32:5085-93. b) May K, Eremin A, Stannarius R, Szabó B, Börzsönyi T, Appel I, et al Exceptionally large magneto-optical response in dispersions of plate-like nanocrystallites and magnetic nanoparticles. J Magn Mater 2017;431:79-83.
- 14. Peroukidis SD, Klapp SHL. Orientational order and translational dynamics of magnetic particle assemblies in liquid crystals. Soft Matter 2016;12:6841-50.
- 15. Nádasi H, Corradi Á, Stannarius R, Koch K, Schmidt AM, Aya S, et al The role of structural anisotropy in the magnetooptical response of an organoferrogel with mobile magnetic nanoparticles. Soft Matter 2019;15:3788-95.
- 16. a) Odenbach S, Thurm S. Magnetoviscous effects in ferrofluids. In: Odenbach S, editor. Ferrofluids: magnetically controllable fluids and their applications. Berlin, Heidelberg: Springer Berlin Heidelberg; 2002:185-201 pp.b) Potisk T, Pleiner H, Svenšek D, Brand HR. Magneto-optic dynamics in a ferromagnetic nematic liquid crystal. Phys Rev E 2018;97:042705-1-13. c) Potisk T, Svenšek D, Pleiner H, Brand HR. Continuum model of magnetic field induced viscoelasticity in magnetorheological fluids. J Chem Phys 2019;150:174901-1-12.
- 17. Arantes FR, Odenbach S. The magnetoviscous effect of micellar solutions doped with water based ferrofluids. J Magn Mater 2015;390:91-5.
- 18. Appel I, Behrens S. Influence of the particle parameters on the stability of magnetic dopants in a ferrolyotropic suspension. J Magn Mater 2017;431:49-53.

- 19. Siboni NH, Shrivastav GP, Klapp SHL. Non-monotonic response of a sheared magnetic liquid crystal to a continuously increasing external field. J. Chem. Phys 2020;152:024505-1-12.
- 20. Liu X, Kent N, Ceballos A, Streubel R, Jiang Y, Chai Y, et al Reconfigurable ferromagnetic liquid droplets. Science 2019;365:264-7.
- 21. Appel I, Nadasi H, Reitz C, Sebastian N, Hahn H, Eremin A, et al Doping of nematic cyanobiphenyl liquid crystals with mesogen-hybridized magnetic nanoparticles. Phys Chem Phys 2017;19:12127-35.
- 22. Prodanov MF, Buluy OG, Popova EV, Gamzaeva SA, Reznikov YO, Vashchenko VV. Magnetic actuation of a thermodynamically stable colloid of ferromagnetic nanoparticles in a liquid crystal. Soft Matter 2016;12:6601-9.
- 23. Gdovinova V, Schroer MA, Tomasovicova N, Appel I, Behrens S, Majorosova J, et al Structuralization of magnetic nanoparticles in 5CB liquid crystals. Soft Matter 2017;13:7890-6.
- 24. Stamatoiu O, Mirzaei J, Feng X, Hegmann T. Nanoparticles in liquid crystals and liquid crystalline nanoparticles. In: Tschierske C, editor. Liquid crystals: materials design and self-assembly. Berlin, Heidelberg: Springer Berlin Heidelberg; 2012:331-93 pp.
- 25. a) Qi H, Kinkead B, Marx VM, Zhang HR, Hegmann T. Miscibility and alignment effects of mixed monolayer cyanobiphenyl liquid-crystal-capped gold nanoparticles in nematic cyanobiphenyl liquid crystal hosts. ChemPhysChem 2009;10:1211-8. b) Draper M, Saez IM, Cowling SJ, Gai P, Heinrich B, Donnio B, et al Self-assembly and shape morphology of liquid crystalline gold metamaterials. Adv Funct Mater 2011;21:1260-78. c) Prodanov MF, Pogorelova NV, Kryshtal AP, Klymchenko AS, Mely Y, Semynozhenko VP, et al Thermodynamically stable dispersions of quantum dots in a nematic liquid crystal. Langmuir 2013;29:9301-9. d) Mirzaei J, Urbanski M, Kitzerow H-S, Hegmann T. Synthesis of liquid crystal silane-functionalized gold nanoparticles and their effects on the optical and electro-optic properties of a structurally related nematic liquid crystal. ChemPhysChem 2014;15:1381-94. e) Feng X, Sosa-Vargas L, Umadevi S, Mori T, Shimizu Y, Hegmann T. Discotic liquid crystal-functionalized gold nanorods: 2- and 3D self-assembly and macroscopic alignment as well as increased charge carrier mobility in hexagonal columnar liquid crystal hosts affected by molecular packing and  $\pi$ - $\pi$  interactions. Adv Funct Mater 2015;25: 1180-92. f) Nealon GL, Greget R, Dominguez C, Nagy ZT, Guillon D, Gallani JL, et al Liquidcrystalline nanoparticles: hybrid design and mesophase structures. Beilstein J Org Chem 2012;8: 349-70. g) Khatua S, Manna P, Chang W-S, Tcherniak A, Friedlander E, Zubarev ER, et al Plasmonic nanoparticles—liquid crystal composites. J Phys Chem C 2010;114:7251-7.
- 26. Nemati A, Shadpour S, Querciagrossa L, Li L, Mori T, Gao M, et al Chirality amplification by desymmetrization of chiral ligand-capped nanoparticles to nanorods quantified in soft condensed matter. Nat Commun 2018;9:3908-1-13.
- 27. a) Kanie K, Sugimoto T. Organic-inorganic hybrid liquid crystals: hybridization of calamitic liquidcrystalline amines with monodispersed anisotropic TiO<sub>2</sub> nanoparticles. J Am Chem Soc 2003;125: 10518-9. b) Kanie K, Muramatsu A. Organic-inorganic hybrid liquid crystals: thermotropic mesophases formed by hybridization of liquid-crystalline phosphates and monodispersed α-Fe<sub>2</sub>O<sub>3</sub> particles. J Am Chem Soc 2005;127:11578–9. c) Saliba S, Coppel Y, Davidson P, Mingotaud C, Chaudret B, Kahn ML, et al Liquid crystal based on hybrid zinc oxide nanoparticles. J Mater Chem 2011;21:6821-3.
- 28. Demortière A, Buathong S, Pichon PB, Panissod P, Guillon D, Bégin-Colin S, et al Nematic-like organization of magnetic mesogen-hybridized nanoparticles. Small 2010;6:1341-6.
- 29. Popova EV, Gamzaeva SA, Krivoshey AI, Kryshtal AP, Fedoryako AP, Prodanov MF, et al Dielectric properties of magnetic nanoparticles' suspension in a ferroelectric liquid crystal. Liq Cryst 2015; 42:334-43.
- 30. a) Sun S, Zeng H, Robinson DB, Raoux S, Rice PM, Wang SX, et al Monodisperse MFe2O4 (M = Fe, Co, Mn) nanoparticles. J Am Chem Soc 2004;126:273-9. b) Behrens S, Essig S. A facile procedure for magnetic fluids using room temperature ionic liquids. J Mater Chem 2012;22:3811-6. c) Essig S,

- Behrens S. Ionic liquids as size- and shape-regulating solvents for the synthesis of cobalt nanoparticles. Chem Ing Tech 2015;87:1741-7. d) Gorschinski A, Khelashvili G, Schild D, Habicht W, Brand R, Ghafari M, et al A simple aminoalkyl siloxane-mediated route to functional magnetic metal nanoparticles and magnetic nanocomposites. J Mater Chem 2009;19:8829-38.
- 31. Liu C, Zou B, Rondinone AJ, Zhang ZJ. Reverse micelle synthesis and characterization of superparamagnetic MnFe<sub>2</sub>O<sub>4</sub> spinel ferrite nanocrystallites. J Phys Chem B 2000;104:1141−5.
- 32. Wang X, Zhuang J, Peng Q, Li Y. A general strategy for nanocrystal synthesis. Nature 2005;437: 121-4.
- 33. Appel I [Ph.D. thesis]. Magnetische Hybridmaterialien auf Basis komplexer, flüssigkristalliner Systeme. Ruprecht-Karls University Heidelberg: Heidelberg; 2017.
- 34. a) Zhou Z, Zhu X, Wu D, Chen Q, Huang D, Sun C, et al Anisotropic shaped iron oxide nanostructures: controlled synthesis and proton relaxation shortening effects. Chem Mater 2015; 27:3505-15. b) Leslie-Pelecky DL, Rieke RD. Magnetic properties of nanostructured materials. Chem Mater 1996;8:1770-83.
- 35. Orlandi S, Benini E, Miglioli I, Evans DR, Reshetnyak V, Zannoni C. Doping liquid crystals with nanoparticles. A computer simulation of the effects of nanoparticle shape. Phys Chem Phys 2016; 18:2428-41.
- 36. Hähsler M, Landers J, Nowack T, Salamon S, Zimmermann M, Heißler S, et al Magnetic properties and Mössbauer spectroscopy of Fe<sub>3</sub>O<sub>4</sub>/CoFe<sub>2</sub>O<sub>4</sub> nanorods. Inorg Chem 2020;59:3677-85.
- 37. Kim D, Lee N, Park M, Kim BH, An K, Hyeon T. Synthesis of uniform ferrimagnetic magnetite nanocubes. J Am Chem Soc 2009;131:454-5.
- 38. a) Ovtar S, Lisjak D, Drofenik M. Barium hexaferrite suspensions for electrophoretic deposition. J Colloid Interface Sci 2009;337:456-63. b) Lisjak D, Jenuš P, Mertelj A. Influence of the morphology of ferrite nanoparticles on the directed assembly into magnetically anisotropic herarchical structures. Langmuir 2014;30:6588-95.
- 39. Pullar RC. Hexagonal ferrites: a review of the synthesis, properties and applications of hexaferrite ceramics. Prog Mater Sci 2012;57:1191-334.
- 40. Hähsler M, Zimmermann M, Heißler S, Behrens S. Sc-doped barium hexaferrite nanodiscs: tuning morphology and magnetic properties. J Magn Mater 2020;500:166349-3-5.
- 41. Hähsler M [Ph.D. thesis]. Responsive magnetische Hybridmaterialienauf Basis funktionalisierter form(an)isotroper Nanopartikel und Flüssigkristalle. Ruprecht-Karls University Heidelberg: Heidelberg; 2020.
- 42. Derouiche Y, Dubois F, Douali R, Legrand C, Maschke U. Some properties of nematic liquid crystal E7/acrylic polymer networks. Mol Cryst Liq Cryst 2011;541:201/[439]-210/[448].
- 43. Gdovinová V, Schroer MA, Tomašovičová N, Appel I, Behrens S, Majorošová J, et al Structuralization of magnetic nanoparticles in 5CB liquid crystals. Soft Matter 2017;13:7890-6.
- 44. Gray GW, Harrison KJ, Nash JA. New family of nematic liquid crystals for displays. Electron Lett 1973;9:130-1.
- 45. Fukuda J-I, Stark H, Yoneya M, Yokoyama H. Interaction between two spherical particles in a nematic liquid crystal. Phys Rev E 2004;69:041706-1-10.
- 46. Kopčanský P, Potočová I, Koneracká M, Timko M, Jansen AGM, Jadzyn J, et al The anchoring of nematic molecules on magnetic particles in some types of ferronematics. J Magn Mater 2005;289: 101-4.
- 47. Muševič I. Nematic liquid-crystal colloids. Materials 2018;11:24.
- 48. a) Reznikov Y. Ferroelectric colloids in liquid crystals. In: Li Q, editor. Liquid crystals beyond displays: chemistry, physics, and applications. John Wiley & Sons: Hoboken, New Jersey; 2012: 403-26 pp.b) Voloschenko D, Pishnyak OP, Shiyanovskii SV, Lavrentovich OD. Effect of director distortions on morphologies of phase separation in liquid crystals. Phys Rev E 2002;65:060701.

- 49. Hähsler M, Behrens S. Dendritic ligands for magnetic suspensions in liquid crystals. Eur J Org Chem 2019;2019:7820-30.
- 50. Prodanov MF, Vashchenko OV, Vashchenko VV. A synthetic strategy toward branched oligomesogenic phosphonic acids: comparison of alternative pathways. Tetrahedron Lett 2014;55: 275-8.
- 51. Dierking I. Textures of liquid crystals. Wiley VCH; WILEY-VCH Verlag GmbH & Co. KGaA, Weinheim;